Tectonophysics 487 (2010) 100–104

Contents lists available at ScienceDirect

Tectonophysics

journal homepage: www.elsevier.com/locate/tecto

Short Communication

One-dimensional dynamical modeling of slip pulses

Chien-chih Chen [a,b,*], Jeen-Hwa Wang [b]

[a] Department of Earth Sciences, National Central University, Jhongli, Taiwan, ROC
[b] Institute of Earth Sciences, Academia Sinica, Nangang, Taipei, Taiwan, ROC

ARTICLE INFO

Article history:
Received 24 December 2009
Received in revised form 5 March 2010
Accepted 15 March 2010
Available online 18 March 2010

Keywords:
Slip pulses
Spring-slider model
Rise time
Duration
Rupture dynamics

ABSTRACT

Propagating slip pulses in earthquake ruptures (Heaton, 1990) are studied based on a one-dimensional N-degree-of-freedom dynamical spring-slider system with a constant ratio of static to dynamic frictional forces. Results show that for almost all cases in the study, the rise time of ruptures at a particular site is much smaller than the duration of ruptures along the whole fault. A propagating slip pulse is generated along the fault. Hence, simulation results are in agreement with Heaton's propagating slip-pulse model.

1. Introduction

Heaton (1990) found that the rise time of a slip at a point on a fault is much shorter than the duration of rupture over the entire fault, and the distribution of rise times over the fault plane is non-uniform. This shows another kind of slip complexity. Since then, several authors also claimed the same observations (Wald et al., 1991; Wald and Heaton, 1994; Nakayama and Takeo, 1997; Nielsen and Madariaga, 2003). Heaton (1990) interpreted the observations using a propagating slip-pulse model (or a self-healing model) with velocity-dependent dynamic friction. In his model, only a relatively small strip, immediately behind the rupture front, slides at any instant. Theoretical studies of the propagating slip pulse were also made by others (Andrews and Ben-Zion, 1996; Beeler and Tullis, 1996; Cochard and Madariaga, 1996; Perrin et al., 1996; Zheng and Rice, 1998; Nielsen et al., 2000; Lapusta et al., 2000; Ben-Zion and Huang, 2002; Nielsen and Madariaga, 2003; Coker et al., 2005; Rice et al., 2005). From the laboratory experiment, Lykotrafitis et al. (2006) observed the self-healing pulse-like shear ruptures. Biegel et al. (2008) studied the effect of off-fault damage on the velocity of a slip pulse from experimental work. In addition to the propagating slip-pulse model, an alternative mechanism to arrest slip of earthquake sources due to geometrical heterogeneity of slip has also been taken into account by some authors. Beroza and Mikumo (1996) stressed that the pre-existing stress and/or strength heterogeneities on the fault plane might provide an adequate geometrical constraint to interpret short rise times. Day et al. (1998) claimed that the self-healing model is not necessary to explain earthquake kinematics. Ide and Takeo (1997) proposed that slip-weakening friction rather than velocity-weakening friction controls fault dynamics. This would imply that velocity-weakening friction is not a factor in producing short rise time.

We here examine the hypothesis of propagating slip pulses in earthquake rupture. Instead of utilizing velocity-dependent dynamic friction, we use a one-dimensional (1D) N-degree-of-freedom spring-slider model (Burridge and Knopoff, 1967), in the presence of constant dynamic friction, to approach this problem.

2. One-dimensional spring-slider model

The 1D N-degree-of-freedom dynamical spring-slider model (Fig. 1) consists of N sliders of equal mass, m, and springs with one slider being linked by a coil spring of strength, K_C, with the other. Each slider is also pulled by a leaf spring of strength, K_L, on a moving plate with a constant velocity, V_p. At time $t=0$, all the sliders rest in the individual equilibrium states. The i-th slider ($i=1, \ldots, N$) is located at position x_i, measured from its initial equilibrium position, along the x-axis. Each slider is subjected to a static frictional force, F_{Si}, at rest. Elastic strain of each slider gradually accumulates due to the moving plate. Once the elastic force at a slider is greater than the static frictional force, the slider will move subject to the dynamic frictional force, F_{Di}. Then the equation of motion for the moving slider is

$$m\left(d^2x_i/dt^2\right) = K_C(x_{i+1}-2x_i+x_{i-1})-K_L\left(x_i-V_pt\right)-F_{Di}. \quad (1)$$

* Corresponding author. Institute of Geophysics, National Central University, Jhongli, Taiwan 320, ROC. Tel.: +886 3 422 7151 65653; fax: +886 3 422 2044.
E-mail address: chencc@ncu.edu.tw (C. Chen).

0040-1951/$ – see front matter © 2010 Elsevier B.V. All rights reserved.
doi:10.1016/j.tecto.2010.03.010

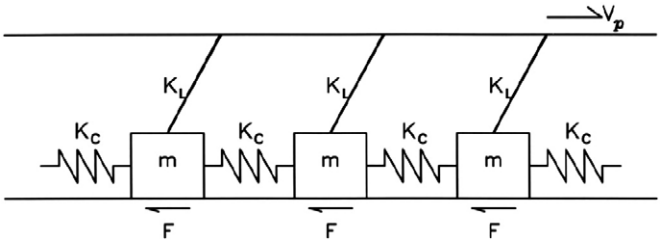

Fig. 1. An N-degree-of-freedom dynamical spring-slider system.

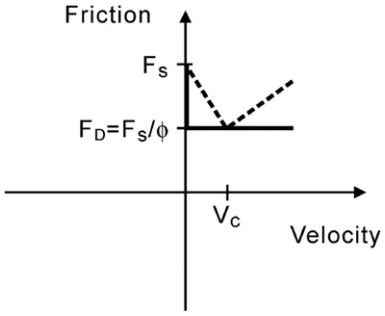

Fig. 2. Schemes for the constant dynamical frictional force (solid line) and the velocity-dependent weakening-hardening frictional force (dashed lines). F_S = the static frictional force; ϕ = the ratio of static to dynamic frictional forces; V_C = the critical velocity having the lowest frictional force.

The classic frictional law with a direct drop of F_{Si} to F_{Di} as displayed by the solid lines in Fig. 2 is considered. Hence, F_{Di} is set to be F_{Si}/ϕ_i. For simplification, only a fixed value of ϕ_i is taken for all sliders in the followings. The plate velocity V_p is usually small and in the order of $\sim 10^{-12}$ m/s.

Eq. (1) can be further normalized by adopting the non-dimensional variables: $S = K_C/K_L$, $\omega_o = (K_L/m)^{1/2}$, and $D_o = F_o/K_L$. Wang (1995) called the quantity S the stiffness ratio. The quantity $\omega_o/2\pi$ is the frequency of oscillation of a single slider attached to a leaf spring in the absence of friction. D_o is the characteristic displacement of a slider exerted by a force F_o through a spring with the strength of K_L. Larger F_o yields longer D_o when K_L is fixed. Obviously, D_o and ω_o are two significant units to scale the spatial coordinates, x_i, and time, t, respectively. Let $X_i = x_i/D_o$ and $\tau = \omega_o t$. This then leads to $dx_i/dt = [F_o/(mK_L)^{1/2}]dX_i/d\tau$, $d^2x_i/dt^2 = (F_o/m)d^2X_i/d\tau^2$, and $V_i = dX_i/d\tau$, together with the normalized (dimensionless) quantities $v_i = V_i/D_o\omega_o$ and $v_p = V_p/D_o\omega_o$. D_o/V_p is the loading time for a leaf spring to stretch enough for overcoming the static frictional force, and v_p is equivalent to the ratio of the slipping time ω_o^{-1} to the loading time. Based on the above-mentioned quantities, Eq. (1) is normalized to the following form:

$$d^2X_i/d\tau^2 = S(X_{i+1} - 2X_i + X_{i-1}) - (X_i - v_p\tau) - F_{Di}/F_o. \quad (2)$$

Two main parameters controlling the motion of a slider are S and v_p. S represents the level of conservation of energy in the system. Larger S shows stronger coupling between two sliders than between a slider and the moving plate. This results in a smaller loss of energy through the K_L spring, thus indicating a higher level of conservation of energy in the system. Since the fault system is a dynamically coupling one with dissipation, S must be a non-zero finite value.

The frictional force is defined only for positive velocities. This means that no backward motions in the fault are allowed. The modeling procedure is simply described here. First, we apply the Runge–Kutta numerical method (Press et al., 1986) to solve Eq. (2) with friction forward in time until all sliders have come to rest. Secondly, we scan all sliders to find the sliders for which the forces are closest to the individual F_{Si}. Thirdly, we add again a loading force from the moving plate to the system, and then repeat the first process. Also, the periodic boundary condition has been utilized to reduce the finite-size effect in numerical calculations.

A modeled event is defined to be a set of connected slipped sliders during a short time interval. Basically, there are small, moderate, and large events. A small event consists of one slipped slider or a few slipped sliders. The moderate event is composed of several tens of sliders. The large event consists of more than 100 sliders. The event which is composed of all sliders is called the system-wide event, which is equivalent to the delocalized event used by Carlson and Langer (1989a,b), hereafter.

3. Results

The value of S, which best models the earthquake fault, has not yet been well determined. Distinct values were used by different authors.

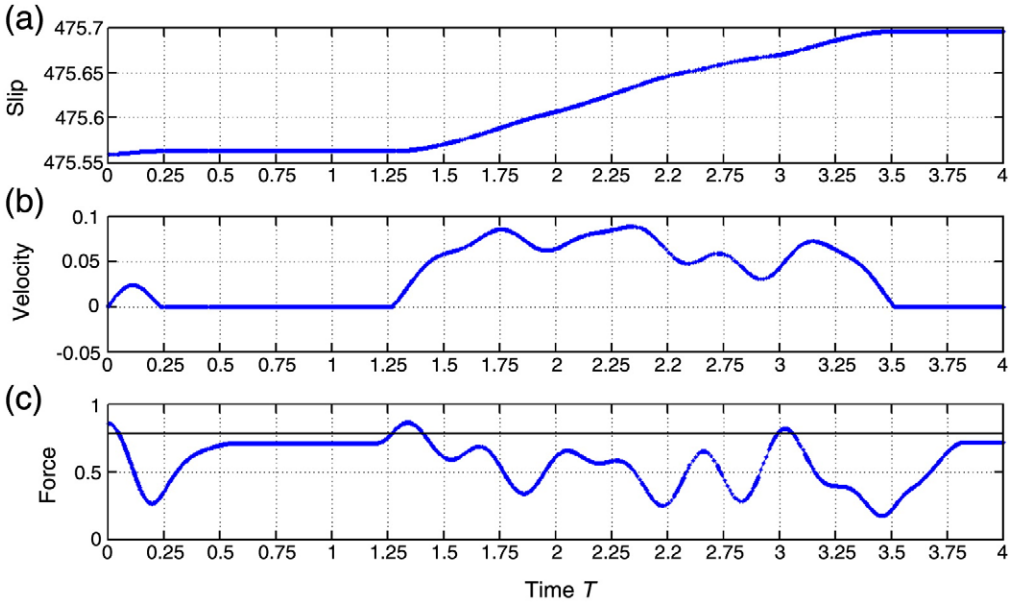

Fig. 3. Temporal variation in (a) slip, (b) velocity, and (c) force at some slipped slider. The horizontal line in the bottom plot denotes the static friction the slider bears. After an early short slip, the slider came to a rest with an elastic force less than the static friction. Then, at $T = \sim 1.25$, the elastic force reached over the level of static friction and the slip occurred again.

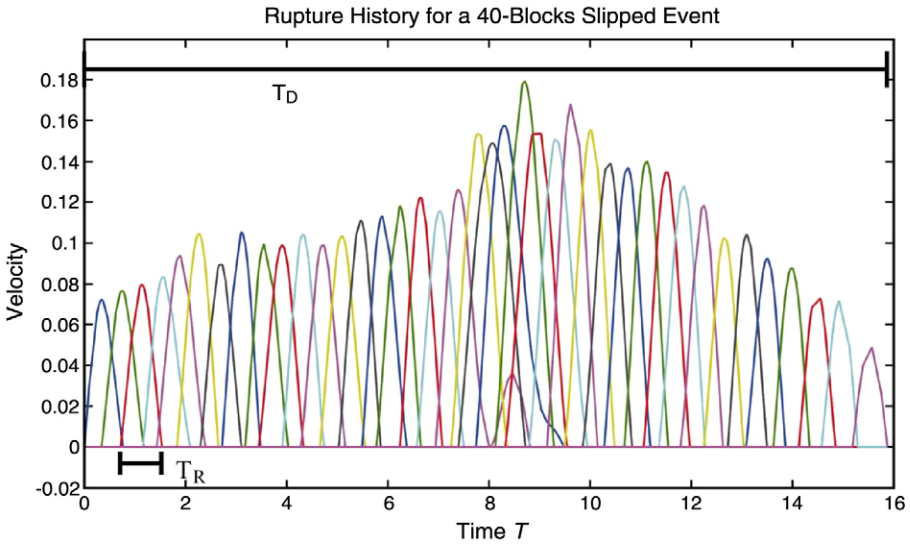

Fig. 4. Temporal variations in velocities at 40 sliders of a moderate event, clearly showing the slip pulse propagating throughout the 40 sliders.

Carlson and Langer (1989a,b) used large values of ~1000. Knopoff et al. (1992) and Xu and Knopoff (1994) used very small values of 0.625 to 2.632. The values of S used by Wang (1991, 1995, 1996, 1997) were less than 120. Based on the frequency–magnitude distribution of synthetic seismicity, Wang (1995) argued that S ranging from 20 to 120 is appropriate for seismicity simulations. Practical tests show that it is hard to generate system-wide events with $S<10$. Since this study mainly focuses on the healing process of large earthquake (Heaton, 1990), two end values of S, i.e., 10 and 100, are thus used in simulations. Throughout this study, the ratio, ϕ, of static to kinetic friction for all sliders is taken as 1.5 and the normalized values, F_{Si}/F_o, of static frictional force are randomly distributed from 0.55 to 1. D_o and ω_o are 1 m and 1 Hz, respectively. The normalized plate velocity v_p is $\sim 10^{-12}$. The number, N, of sliders is 2^7 (=128).

An example showing the temporal variations in slip, velocity, and force at slipped sliders is given in Fig. 3 when $S=100$. The slider shown in Fig. 3 had experienced two steps of slip during a multiple-slipped-sliders event. In the first step, the slip is in general quite simple and shows a sinusoidal-function form (i.e., the first waveform from $T=0$ through $T=0.25$ in Fig. 3b). However, in the second step, the slip (i.e. the second waveform from $T=1.25$ through $T=3.5$ in Fig. 3b) becomes very complicated due to complexity of the N-degree-of-freedom system.

Fig. 4 is an example of the temporal variations in velocities at 40 sliders of an event and shows the rupture process of the event. The rupture is composed of numerous slip pulses, which propagate outwards from the site with the lowest value of F_S, and stop at the site with larger F_S. This figure also demonstrates the definition of the rise time, T_R, of a slip pulse and the duration, T_D, of the whole rupture. T_R is the time span within which the velocity first increases from zero to the peak and then decreases from the peak to zero. T_D is the time interval from the starting time of the first slip pulse to the ending time of the last slip pulse. It is obvious that T_R is much smaller than T_D.

Fig. 5 shows the probability density functions (PDF) of T_R/T_D for $S=10$ (in the dashed lines) and 100 (in the solid lines), respectively. Meanwhile, blue color and red color are used for the system-wide and

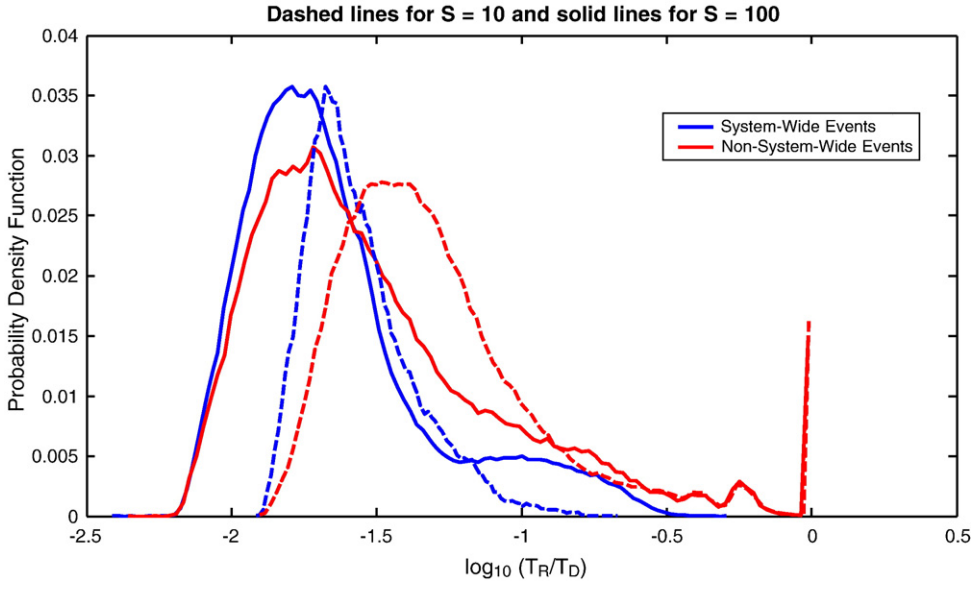

Fig. 5. The probability density functions (PDF) of T_R/T_D for $S=10$ and 100. Note that the horizontal axis is in the logarithmic scale. For details please refer to the text.

non-system-wide events, respectively. In general the values of PDF first increases with $\log_{10}(T_R/T_D)$ from zero to a peak and then decreases with increasing $\log_{10}(T_R/T_D)$ from the peak to zero. However, for the non-system-wide events, there is a second peak near $\log_{10}(T_R/T_D)\approx 0$ or $T_R/\approx 1$. For both the system-wide and non-system-wide events, the PDF for $S=10$ moves to the right of that for $S=100$. The PDF's for $S=100$ are similar to each other, while those for $S=10$ are slightly different.

4. Discussion

Fig. 5 obviously shows that considering the non-system-wide events as depicted by red dashed and solid lines, except for the spiky tails with $T_R/T_D\approx 1$, T_R/T_D is much smaller than 1. It seems reasonable that for small events with one slipped slider, T_R is comparable to T_D, i.e., $T_R/T_D\approx 1$ as expected, whatever the model parameters are. For the small events, the occurrence times of the sliders are close to one another and the number of connected slipped sliders is small. Thus, T_D cannot be much larger than T_R of the individual slider. In other words, T_R/T_D is less than but close to 1. Except for the small events, T_R/T_D is low. For example, 99% of T_R/T_D of the system-wide events when $S=10$ are lower than 0.1 (Fig. 5). This is essentially similar to the observation obtained by Heaton (1990). A slip pulse propagating outwards from the initial breaking point (see Fig. 4) is also consistent with that done theoretically by the above-mentioned authors.

As shown in Fig. 5, the statistical distributions of T_R/T_D for both $S=10$ and 100 are much like the log-normal distribution specified with a mode ≤ 0.03. The distribution of non-system-wide events for $S=10$ (in the red dashed line) shows a slightly higher mode of ~0.03, while the other three distributions with the modes <0.03 are close to one another. In other words, the mode of the statistical distribution of T_R/T_D only slightly decreases with increasing S. Hence, the stiffness ratio is only a minor factor in affecting the distribution of T_R/T_D.

Friction is a very complicated physical process. Dieterich (1979) found velocity-dependence of dynamic friction. Ruina (1983) proposed empirical velocity- and state-dependent friction laws. Essentially, the velocity-dependent friction law includes two processes: the velocity-weakening process and the velocity-hardening one. For the first-order approximation, Wang (1991) considered a piece-wise, linearly velocity-dependent weakening-hardening friction law (displayed by the dashed lines in Fig. 2). This is consistent with the experimental result (cf. Tsutsumi and Shimamoto, 1997) that the frictional force first decreases with increasing velocity at low velocities and then increases with velocity at high velocities. The constant dynamic friction as shown by the solid lines in Fig. 2 represents the limit case of weakening, with an infinite rate, excluding hardening. A sudden drop of static to dynamic frictional forces behaves like an extra force to push the slider move, and means that no fracture energy is needed to promote faulting. While a finite amount of fracture energy is requested to promote faulting for the velocity-weakening frictional force. Hence, rapidly weakening in the dynamic friction could be easier to increase the time of motion of a slider, thus lengthening T_R, than slowly weakening. On the other hand, a constant dynamic friction force would be more efficient to retain the motion of the slider than an increasing dynamic frictional force with velocity as proposed by Wang (1991). Rapidly hardening in or suddenly increasing the dynamic frictional force will be more capable of resisting the motion of a slider than slowly hardening, leading to shorter T_R. Therefore, the value of T_R/T_D for the velocity-dependent weakening-hardening friction law is expected to be shorter than that of this study. This makes self-healing slip pulses exist.

5. Conclusions

On the basis of the simulations of a 1D N-degree-of-freedom dynamical spring-slider model, we explore the possible existence of propagating slip pulse in earthquake rupture and study the ratio T_R/T_D. Simulation results show the existence of the propagating slip pulse. The values of T_R/T_D estimated from this study with constant dynamic friction are usually smaller than 0.1. This suggests that the duration of slip at a given point on a fault is in general as short as 10% of the overall duration of an earthquake. The present results are essentially comparable with the propagating slip pulse observed by and related model proposed by Heaton (1990). We furthermore conjecture that adopting the velocity-weakening-and-hardening friction law, which is a widely accepted form in friction, seems to be more robust for interpreting the small rise times than the present study of adopting the constant dynamic friction.

Acknowledgments

CCC is grateful for the research support from both the National Science Council (ROC) and the Institute of Geophysics (NCU, ROC). This study was financially supported by the Academia Sinica and the National Sciences Council, ROC under Grant No. NSC96-2116-M-001-012-MY3.

References

Andrews, D.J., Ben-Zion, Y., 1996. Wrinkle-like slip pulse on a fault between different materials. J. Geophys. Res. 102, 553–571.
Beeler, N.M., Tullis, T.E., 1996. Self-healing slip pulses in dynamic rupture models due to velocity-dependent strength. Bull. Seismol. Soc. Am. 86, 1130–1148.
Ben-Zion, Y., Huang, Y., 2002. Dynamic rupture on an interface between a compliant fault zone layer and a stiffer surrounding solid. J. Geophys. Res. 107 (B2). doi:10.1029/2001JB000254.
Beroza, G.C., Mikumo, T., 1996. Short slip duration in dynamic rupture in the presence of heterogeneous fault properties. J. Geophys. Res. 101, 22449–22460.
Biegel, R.L., Sammis, C.G., Rosakis, A.J., 2008. An experimental study of the effect of off-fault damage on the velocity of a slip pulse. J. Geophys. Res. 113, B04302. doi:10.1029/2007JB005234.
Burridge, R., Knopoff, L., 1967. Model and theoretical seismicity. Bull. Seismol. Soc. Am. 57, 341–371.
Carlson, J.M., Langer, J.S., 1989a. Properties of earthquakes generated by fault dynamics. Phys. Rev. Lett. 62, 2632–2635.
Carlson, J., Langer, J.S., 1989b. Mechanical model of an earthquake fault. Phys. Rev. A 40, 6470–6484.
Cochard, A., Madariaga, R., 1996. Complexity of seismicity due to highly rate-dependent friction. J. Geophys. Res. 101, 25321–25336.
Coker, D., Lykotrafitis, G., Needleman, A., Rosakis, A.J., 2005. Frictional sliding modes along an interface between identical elastic plates subject to shear impact loading. J. Mech. Phys. Solids 53, 884–922.
Day, S.M., Yu, G., Wald, D.J., 1998. Dynamic stress changes during earthquake rupture. Bull. Seismol. Soc. Am. 88, 512–522.
Dieterich, J.H., 1979. Modeling of rock friction 1. Experimental results and constitutive equations. J. Geophys. Res. 84, 2161–2168.
Heaton, T.H., 1990. Evidence for and implications of self-healing pulses of slip in earthquake rupture. Phys. Earth Planet. Int. 64, 1–20.
Ide, S., Takeo, M., 1997. Determination of constitutive relations of fault slip based on seismic wave analysis. J. Geophys. Res. 102, 27379–27391.
Knopoff, L., Landoni, J.A., Abinante, M.S., 1992. Dynamical model of an earthquake fault with localization. Phys. Rev. A 46, 7445–7449.
Lapusta, N., Rice, J.R., Ben-Zion, Y., Zheng, G., 2000. Elastodynamic analysis for slow tectonic loading with spontaneous rupture episodes on faults with rate- and state-dependent friction. J. Geophys. Res. 105, 23765.
Lykotrafitis, G., Rosakis, A.J., Ravichandran, G., 2006. Self-healing pulse-like shear ruptures in the laboratory. Science 313, 1765–1768.
Nakayama, W., Takeo, M., 1997. Slip history of the 1994 Sanriku-Haruka-Oki, Japan, earthquake deduced from strong-motion data. Bull. Seismol. Soc. Am. 87, 918–931.
Nielsen, S., Madariaga, R., 2003. On the self-healing fracture model. Bull. Seismol. Soc. Am. 93, 2375–2388.
Nielsen, S.B., Carlson, J.M., Olsen, K.B., 2000. Influence of friction and fault geometry on earthquake rupture. J. Geophys. Res. 105, 6069.
Perrin, G., Rice, J.R., Zheng, G., 1996. Self-healing slip pulse on a friction surface. J. Mech. Phys. Solids 43, 1461–1495.
Press, W.H., Flannery, B.P., Teukolsky, S.A., Vetterling, W.T., 1986. Numerical Recipes. Cambridge Univ. Press, Cambridge. 818 pp.
Rice, J.G., Sammis, C.G., Parsons, R., 2005. Off-fault second failure induced by a dynamic slip pulse. Bull. Seismol. Soc. Am. 95, 109–134.
Ruina, A.L., 1983. Slip instability and state variable friction laws. J. Geophys. Res. 88, 10,359–10,370.
Tsutsumi, A., Shimamoto, T., 1997. High-velocity frictional properties of gabbro. Geophys. Res. Lett. 24, 699–702.
Wald, D.J., Heaton, T.H., 1994. Spatial and temporal distribution of slip for the 1992 Landers, California, earthquake. Bull. Seismol. Soc. Am. 84, 668–691.

Wald, D.J., Helmberger, D.V., Heaton, T.H., 1991. Rupture model of the 1989 Loma Prieta earthquake from the inversion of strong-motion and broadband teleseismic data. Bull. Seismol. Soc. Am. 81, 1540–1572.
Wang, J.H., 1991. A note on the correlation between b-value and fractal dimension from synthetic seismicity. Terr. Atmos. Ocean. Sci. 2, 317–329.
Wang, J.H., 1995. Effect of seismic coupling on the scaling of seismicity. Geophys. J. Int. 121, 475–488.
Wang, J.H., 1996. Velocity-weakening friction as a factor in controlling the frequency-magnitude relation of earthquakes. Bull. Seismol. Soc. Am. 86, 701–713.
Wang, J.H., 1997. Effect of frictional healing on the scaling of seismicity. Geophys. Res. Lett. 24, 2527–2530.
Xu, H.J., Knopoff, L., 1994. Periodicity and chaos in a one-dimensional dynamical model of earthquakes. Phys. Rev. 50, 3577–3581.
Zheng, G., Rice, J.R., 1998. Conditions under which velocity-weakening friction allows a self-healing versus a cracklike mode of rupture. Bull. Seismol. Soc. Am. 88, 1466–1483.